Supporting Information

Polyhedral oligosilsesquioxane tethered perylene diimide for application in optical limiting and rapid detection of fluoride ions

Tian Gao,[a] Wen-Fa Zhou,[b] Yang Zhao,[a] Lei Shen,[b] Wen-Ying Chang,[c] Rodney-Kudzai Musendo,[a] Er-Qiang Chen,[c] Ying-Lin Song*[b] and Xiang-Kui Ren*[a]

[a]School of Chemical Engineering and Technology, Tianjin University, Tianjin 300350, P. R. China.

[b]School of Physical Science and Technology, Soochow University, Suzhou 215006, P. R. China.

[c]Beijing National Laboratory for Molecular Sciences, College of Chemistry, Peking University, Beijing 100871, P. R. China.

Section 1. Materials and Methods

Perylene-3,4,9,10-tetracarboxylic acid dianhydride (PDA, 98%) was purchased from Beijing HWRK company, and p-Aminopropylisobutyl POSS (AM0292, ⩾97%) was purchased from Hybrid Plastics. All the other chemicals were purchased from Jiangtian Chemical Reagents Co. Ltd. and directly used without further purification.

^{1}H, ^{13}C and ^{29}Si NMR spectra of the samples were recorded with a Bruker Avance 400 spectrometer at 298 K using deuterated chloroform ($CDCl_3$) as the solvent and tetramethylsilane (TMS) as the internal standard. High resolution mass spectra (HRMS) were determined on an IonSpec 4.7 Tesla Fourier Transform Mass Spectrometer. Fourier transform infrared spectroscopy (FT-IR) was performed with a Perkin-Elmer FTIR-100 spectrometer. UV/Vis absorption spectra were recorded on a Mapada UV-3200 spectrophotometer. Fluorescence spectra were obtained on a Hitachi FL-2500 luminescence spectrometer.

In order to investigate the nonlinear optical response of the two compounds, femtoseconds Z-scan experiments (light source: OPA, Light Conversion ORPHEUS, 190 fs, 20 Hz) at 600 nm were conducted. The incident pulse laser was divided two parts, one

is used to monitor the energy fluctuation of the incident pulse laser and the other is focused by a focusing lens. The sample was placed at the precision mobile platform near the focal plane and moved along the direction of Z (the direction of laser propagation). Finally, two energy probes were used to record the laser energy variation.

Section 2. Synthesis

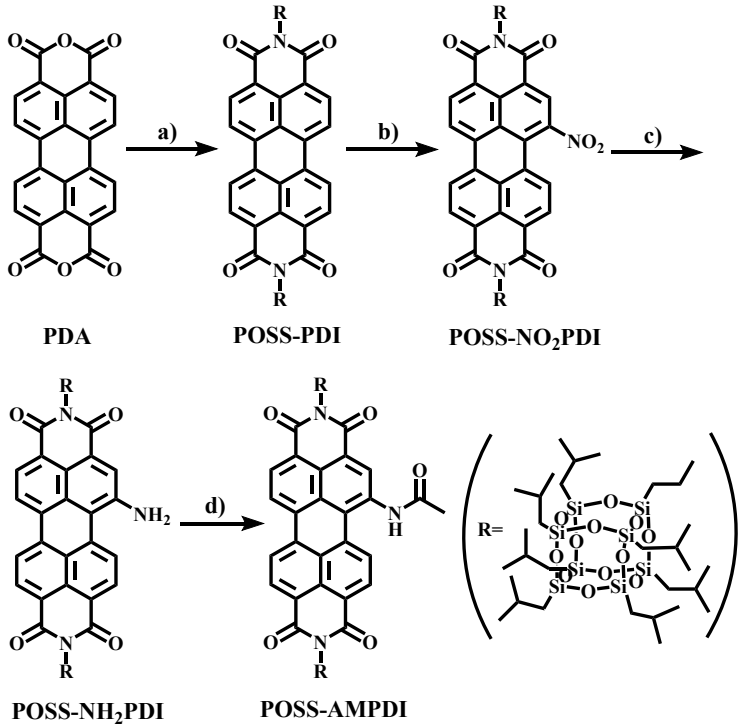

Scheme S1. Synthetic routes of POSS-AMPDI. (a) NH_2-R, imidazole, 140 °C; (b) nitrosonitric acid, dichloromethane, 0 °C; (c) zinc powder, glacial acetic acid, tetrahydrofuran, room temperature; (d) acetyl chloride, pyridine, tetrahydrofuran.

Compound POSS-PDI

30.00 g of imidazole was placed in a 100 mL round-bottom flask and completely melt at 120 °C, then PDA (1.00 g, 2.55 mmol) and p-Aminopropylisobutyl POSS (5.36 g, 6.12 mmol) were added with stirring. The mixture was heated to 140 °C and reflux for 4 h. Upon cooling, the mixture was poured into 300 mL of methanol and stirred for few hours to remove the imidazole. Then the mixture was filtered and the precipitate was washed using

methanol. After dried at 50 °C under vacuum oven, the crude product was purified by column chromatography on silica gel (dichloromethane/ethyl acetate = 1:6, V/V) to give an orange solid (95%). ^{1}H NMR (400 MHz, $CDCl_3$) δ (TMS, ppm): 8.67 (s, 4H, ArH), 8.59 (s, 4H, ArH), 4.21 (t, 4H, -N-CH_2-), 1.85 (m, 18H, -CH- and -CH_2-), 0.94 (m, 84H, -CH_3), 0.72 (t, 4H, -CH2-), 0.59 (m, 28H, -CH_2-). ^{13}C NMR (400 MHz, $CDCl_3$) δ (TMS, ppm): 163.00, 134.18, 131.06, 129.10, 126.08, 123.25, 122.81, 42.95, 25.70, 23.88, 22.50, 21.57, 9.79. HRMS (MALDI (N), 100%) m/z calcd for $C_{86}H_{146}N_2O_{28}Si_{16}$: 2102.6375, found 2102.6372.

Compound POSS-NO_2PDI

POSS-PDI (1.00 g, 0.48 mmol), dichloromethane (40 mL) were placed in a 100 mL round-bottom flask and stirred in ice bath for few minutes, then a previously prepared solution of dichloromethane (5 mL) containing 2 mL of nitrosonitric acid was added dropwise to the above solution under stirring. After about 1 hour, the mixture was poured into 300 mL of methanol and stirred for two hours. The precipitate was filtered and then dried at 50 °C under vacuum oven. The crude product was purified by column chromatography on silica gel (dichloromethane/ethyl acetate = 1:1, V/V) to give an red solid (98%). ^{1}H NMR (400 MHz, $CDCl_3$) δ (TMS, ppm): 8.79 (s, 5H, ArH), 8.66 (s, 1H, ArH), 8.30 (s, 1H, ArH), 4.24 (t, 4H, -N-CH_2-), 1.84 (m, 18H, -CH- and –CH_2-), 0.97 (m, 84H, -CH_3), 0.72 (t, 4H, -CH_2-), 0.60 (m, 28H, -CH_2-). ^{13}C NMR (400 MHz, $CDCl_3$) δ (TMS, ppm): 162.78, 162.49, 162.37, 161.58, 147.52, 135.37, 132.83, 132.67, 131.22, 131.04, 129.26, 129.15, 128.77, 127.88, 127.37, 126.51, 126.31, 126.18, 124.81, 124.44, 124.09, 123.98, 123.84, 123.02, 43.18, 25.70, 23.88, 22.50, 21.49, 9.75. HRMS (MALDI (N), 100%) m/z calcd for $C_{86}H_{145}N_3O_{30}Si_{16}$: 2147.6226, found 2147.6238.

Compound POSS-NH_2PDI

To a 100 mL round-bottom flask, POSS-NO_2PDI (0.5 g, 1.6 mmol), Zn powder (0.9 g, 15 mmol), ethylic acid (3 mL, 50 mmol) and 20 mL tetrahydrofuran were added. The reaction

mixture was stirred for 24 h at room temperature and then the zinc powder was removed by filtration. After the removal of the tetrahydrofuran, the crude product was dissolved in dichloromethane and washed with 5% NaOH (w/w) aqueous solution. After the solvent was removed, the obtained solid was was purified by column chromatography on silica gel (dichloromethane/ethyl acetate = 2:1, V/V) to give an purple solid (68%). ^{1}H NMR (400 MHz, $CDCl_3$) δ (TMS, ppm): 8.89 (d, 1H, ArH), 8.68 (m, 2H, ArH), 8.52 (m, 3H, ArH), 8.18 (s, 1H, ArH), 5.17 (s, 2H, -NH_2), 4.21 (m, 4H, -N-CH_2-), 1.86 (m, 18H, -CH- and –CH_2-), 0.95 (m, 84H, -CH_3), 0.76 (t, 4H, -CH_2-), 0.60 (m, 28H, -CH_2-). ^{13}C NMR (400 MHz, $CDCl_3$) δ (TMS, ppm): 163.50, 163.41, 163.12, 162.95, 145.93, 136.12, 135.00, 132.68, 131.41, 130.92, 129.31, 128.25, 127.23, 127.17, 125.06, 123.99, 123.73, 123.54, 123.03, 122.80, 121.97, 121.04, 120.51, 111.60, 42.87, 25.71, 23.88, 22.50, 21.51, 9.82. HRMS (MALDI (N), 100%) m/z calcd for $C_{86}H_{147}N_3O_{28}Si_{16}$: 2117.6484, found 2117.6471.

Compound POSS-AMPDI

A mixture of POSS-NH_2PDI (0.2 g, 0.095 mmol) and 2 mL of pyridine was dissolved in 20 mL of tetrahydrofuran and then cooled in ice bath. Afterward, a previously prepared solution of tetrahydrofuran (5 mL) containing 1.5 mL of acetyl chloride was added dropwise to the above solution with stirring. 30 minutes later, the reaction mixture was moved to room temperature and kept stirring for 24 hours. After the solvent was removed, The crude product was purified by silica gel column chromatography with (dichloromethane/ethyl acetate = 2:1, V/V) as eluent to give an red solid (33%). ^{1}H NMR (400 MHz, $CDCl_3$) δ (TMS, ppm): 8.93 (s, 1H, -NH-), 8.85 (s, 1H, ArH), 8.66-8.34 (m, 5H, ArH), 8.11 (s, 1H, ArH), 4.21 (s, 4H, -N-CH_2-), 2.43 (s, 3H, -CH_3), 1.86 (m, 18H, -CH- and -CH_2-), 0.96 (m, 84H, -CH_3), 0.83-0.69 (m, 4H, -CH_2-), 0.61 (m, 28H, -CH_2-). ^{13}C NMR (400 MHz, $CDCl_3$) δ (TMS, ppm): 169.44, 163.25, 162.56, 162.06, 135.34, 133.79, 133.32, 131.78, 130.42, 130.37, 130.19, 130.14, 129.73, 128.27, 127.79, 127.52, 127.17, 126.45, 126.15, 125.55, 123.27, 122.93, 121.46, 120.45, 42.92, 25.50, 23.67,

22.28, 21.29, 9.70, 9.56. HRMS (MALDI (N), 100%) m/z calcd for $C_{88}H_{149}N_3O_{29}Si_{16}$: 2159.6590, found 2159.6580.

Section 3. Photophysical Properties

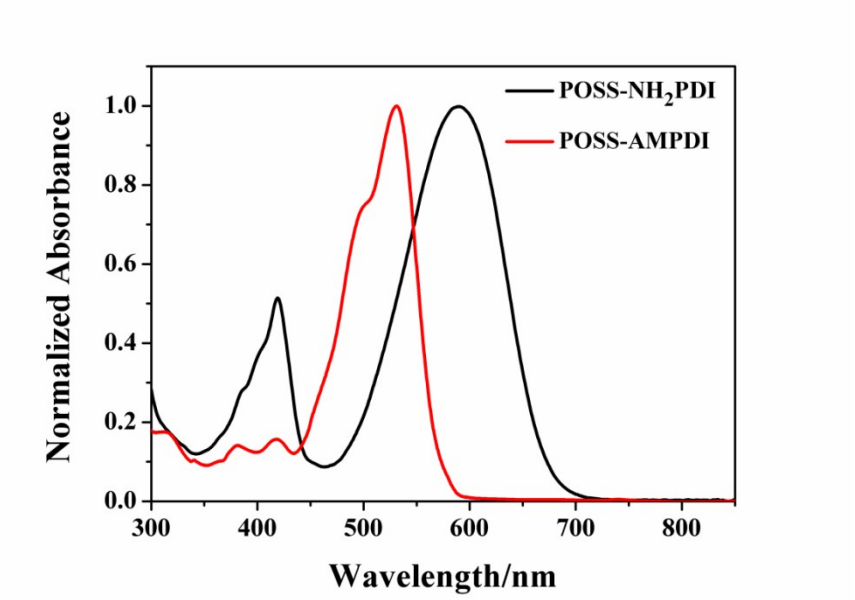

Fig. S1 UV/Vis absorption spectra of POSS-NH_2PDI and POSS-AMPDI.

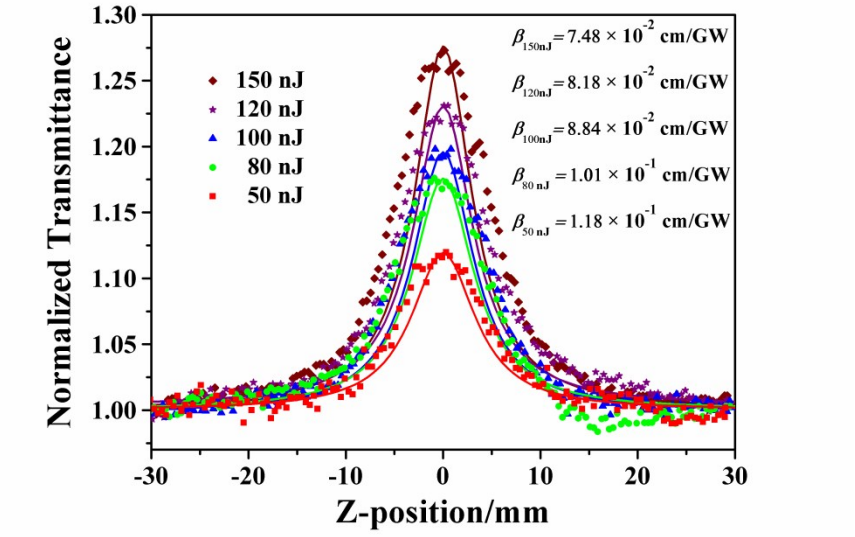

Fig. S2 Open-aperture Z-scan curves of POSS-NH_2PDI for different input intensities at 600 nm with 190-fs pulses. Solid lines represent the theoretical fitting curves.

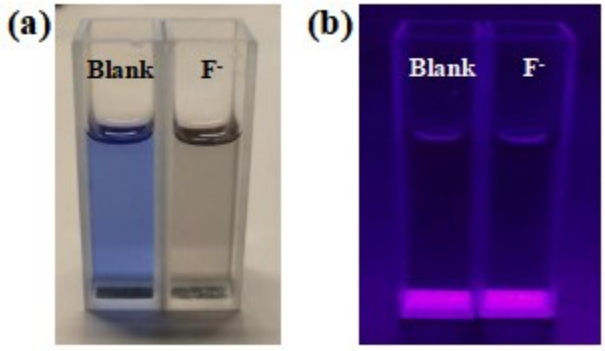

Fig. S3 The color change of POSS-NH_2PDI after the addition of F^-. (a) in the sunlight; (b) by UV irradiation of 365 nm.

Section 4. Detection limit

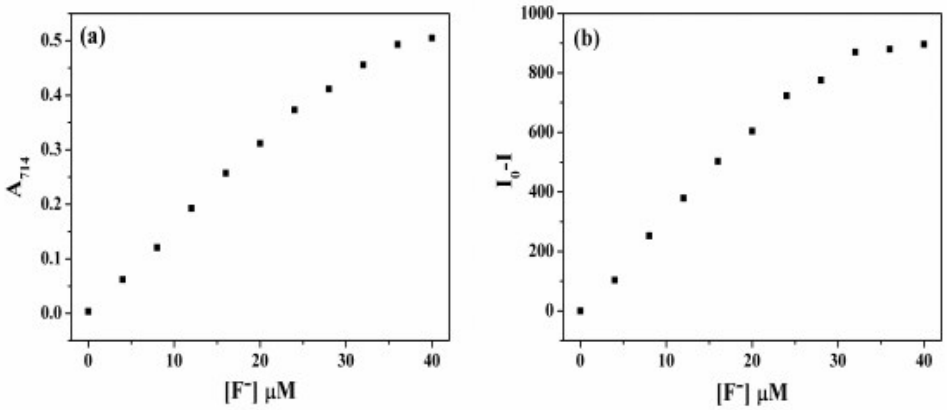

Fig. S4 (a) Plot of the absorbance of POSS-AMPDI at 714 nm (A_{714}) in the presence of different concentrations of fluoride ions. (b) Plot of the emission intensity of POSS-AMPDI at 594 nm (I_0-I, I_0 represents the fluorescence intensity without fluoride ions, I represents the fluorescence intensity with corresponding amounts of fluoride ions) in the presence of different concentrations of fluoride ions. The detection limit of fluoride anions was calculated according to the IUPAC equation: $C_L=K*\sigma/S$, K represents a constant related to confidence (K=3), σ represents the standard deviation of the blank value

(σ=8.23273×10^{-5}), S represents the slope of the curve over the low concentration range in Fig. S2a (S=15028.57143). The detection limit was calculated to be 1.64×10^{-8} M.

Section 5. Selectivity investigation

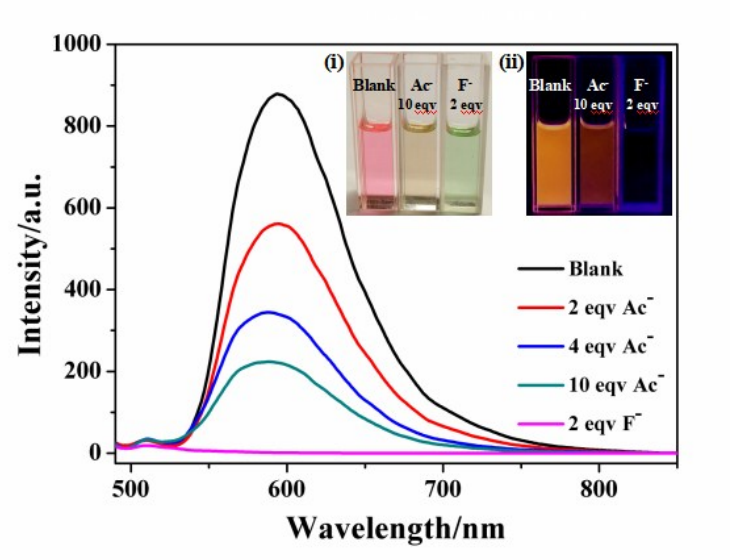

Fig. S5 The fluorescence spectra of POSS-AMPDI in THF with the presence of different amount of Ac^- and F^-. Inset: The color and optical changes in fluorescence emission of POSS-AMPDI after the addition of 10 equiv. Ac^- and 2 equiv. F^- (i : in the sunlight; ii : by UV irradiation of 365 nm).

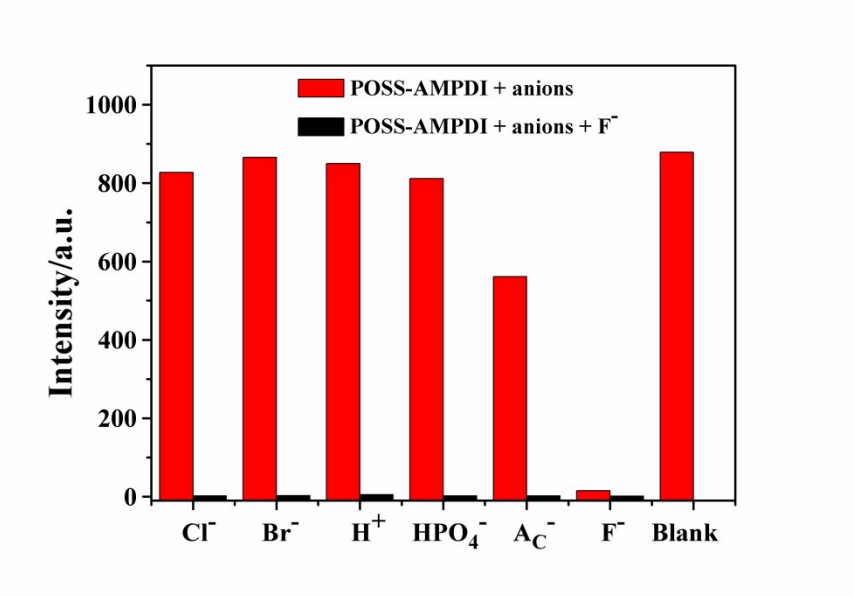

Fig. S6 Emission intensity of POSS-AMPDI in the presence of a single anion (red bars) and in the mixture of F^- and other anions (black bars). Solvent: THF, [POSS-AMPDI] = 20 μM, [anions] = 40 μM.

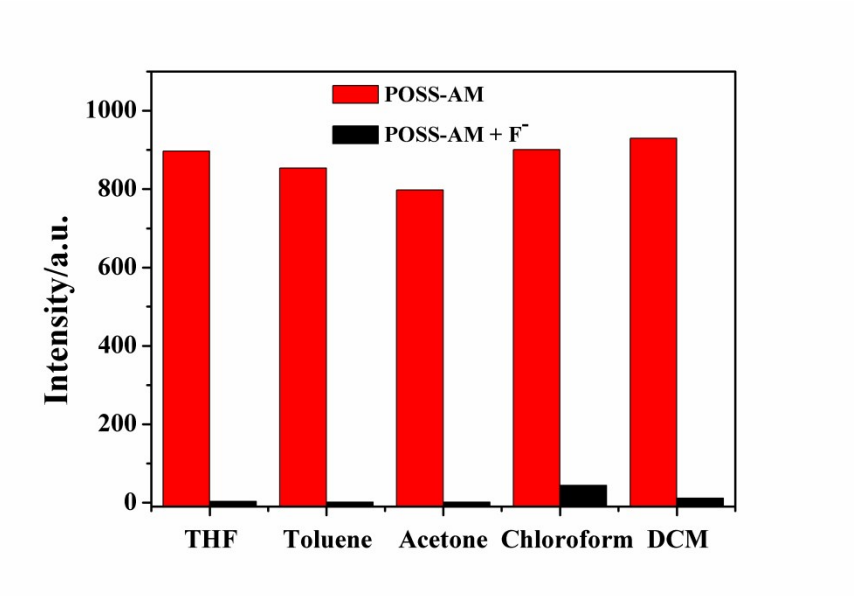

Fig. S7 Emission intensity of POSS-AMPDI in the mixed solvent of THF with other solvents (v/v=1/1, red bars) and in the presence of 2 equiv. of F^- (black bars).

Section 6. Sensing mechanism

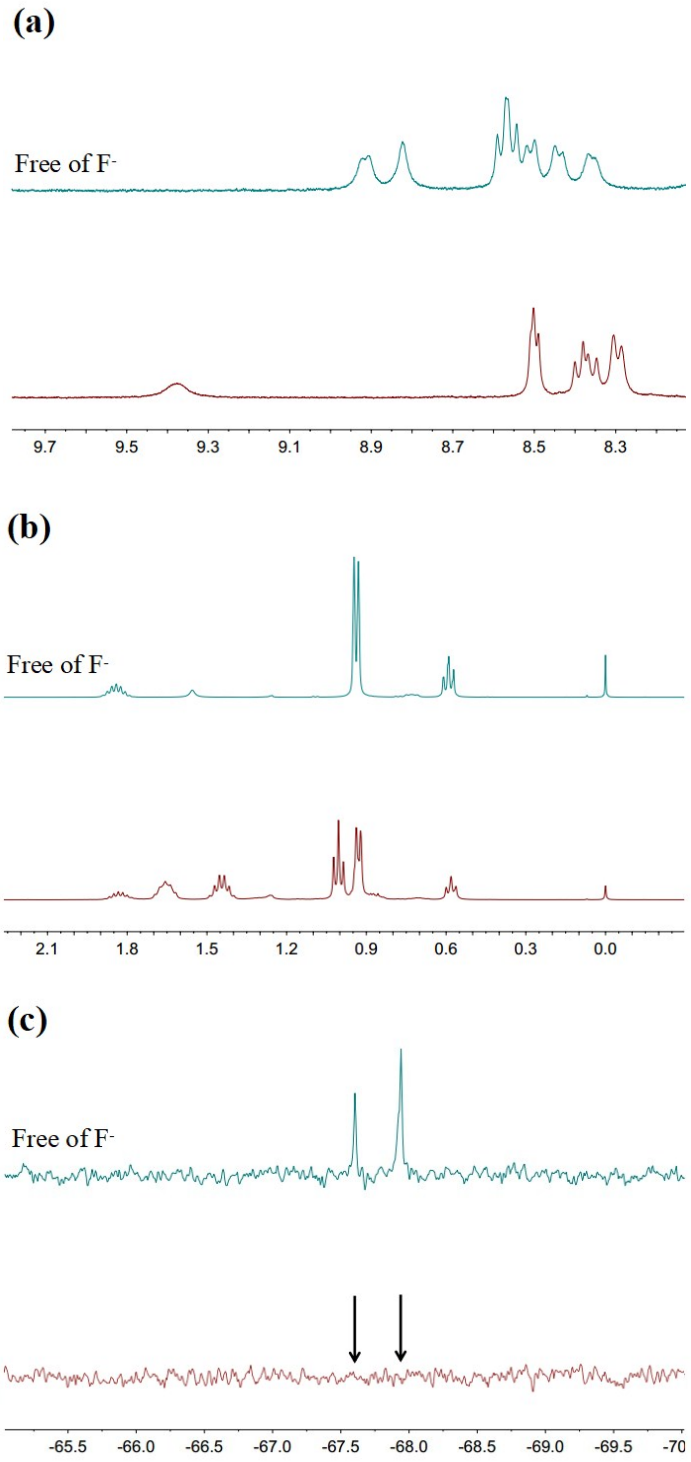

Fig. S8 (a) ^{1}H NMR spectra (ranged 8.1-9.7 ppm) of POSS-AMPDI in $CDCl_3$ (upper) and the solute after the addition of 2 equiv. TBAF (below). (b) ^{1}H NMR spectra (ranged 0-2.1 ppm) of POSS-AMPDI in $CDCl_3$ (upper) and the solute after the addition of 2 equiv. TBAF (below). The peaks corresponding to aromatic protons (between 8.25 to 8.60 ppm) changed to some extent. This may be related to both the PDI electric cloud distribution distortion induced by the N-H deprotonation and the PDI aggregation induced by POSS collapse. The peaks corresponding to isobutyl and Si-CH_2 of POSS (between 0.5 to 2.0 ppm) also exhibit distinct change, indicating the fluoride-triggered POSS collapse. (c) ^{29}Si NMR spectra of POSS-AMPDI in $CDCl_3$ (upper) and the solute after the addition of 2 equiv. TBAF (below) in $CDCl_3$.

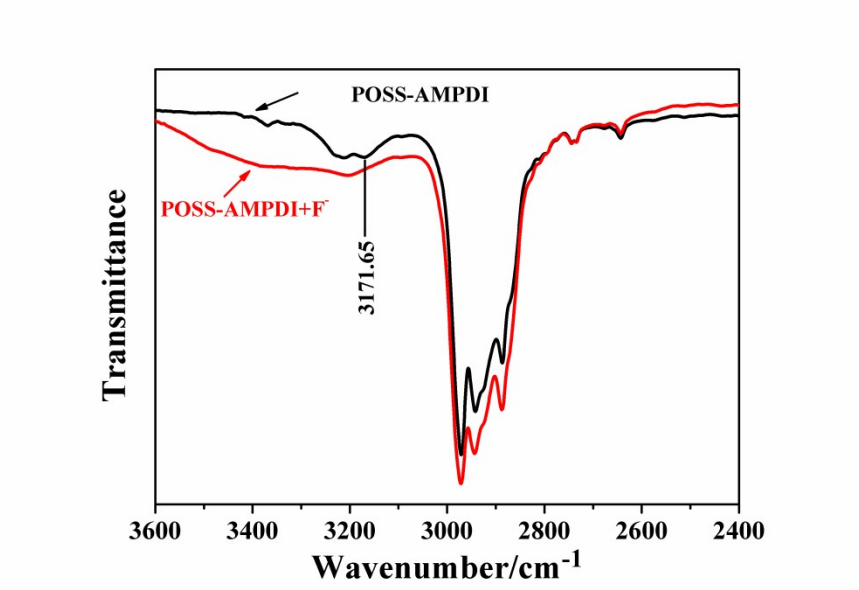

Fig. S9 Partial infrared spectra of POSS-AMPDI in the presence of 0 and 2 equiv. of F^-.

Section 7. Z-scan curves of POSS-AMPDI after the addition of F^-

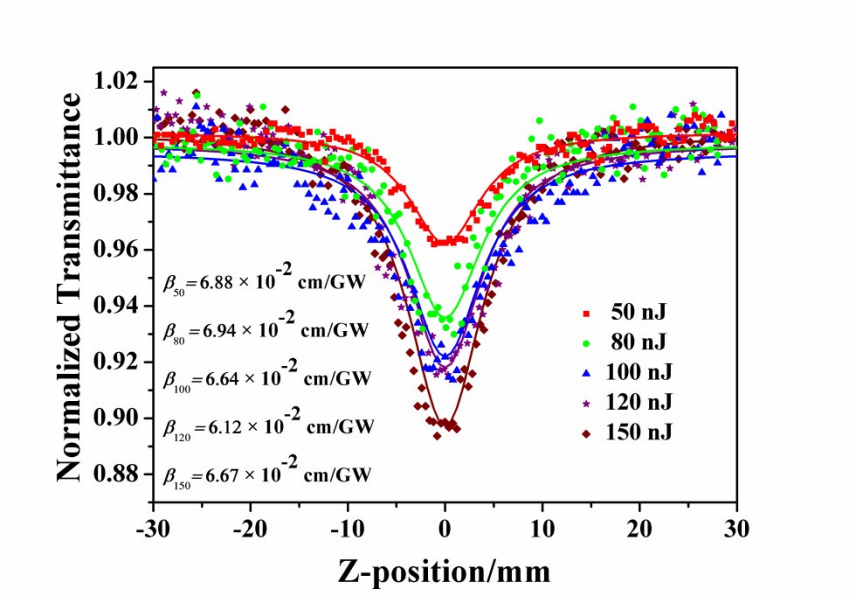

Fig. S10 Open-aperture Z-scan curves of POSS-AMPDI for different input intensities at 600 nm after the addition of F^-. Solid lines represent the theoretical fitting curves.

Section 8. NMR Spectra

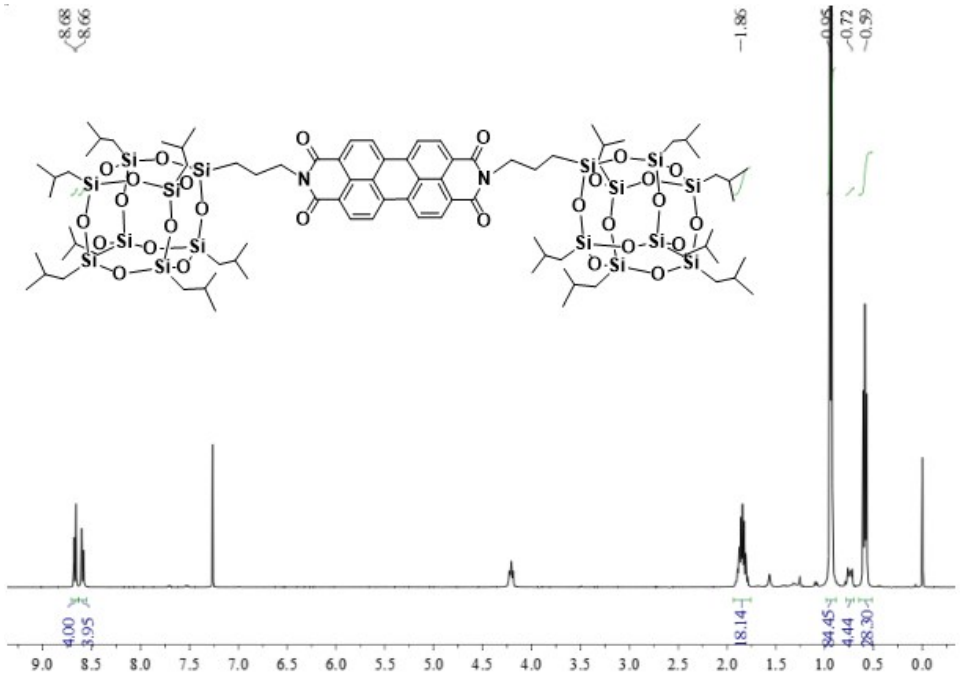

Fig. S11 ^1H NMR spectrum of POSS-PDI recorded in $CDCl_3$.

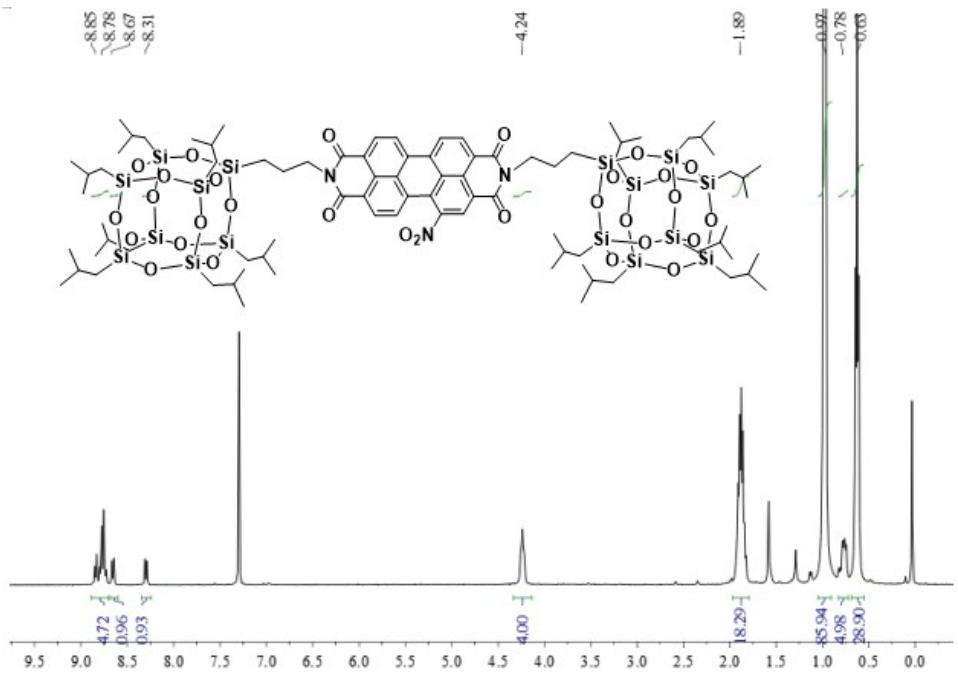

Fig. S12 ^{1}H NMR spectrum of POSS-NO_2PDI recorded in $CDCl_3$.

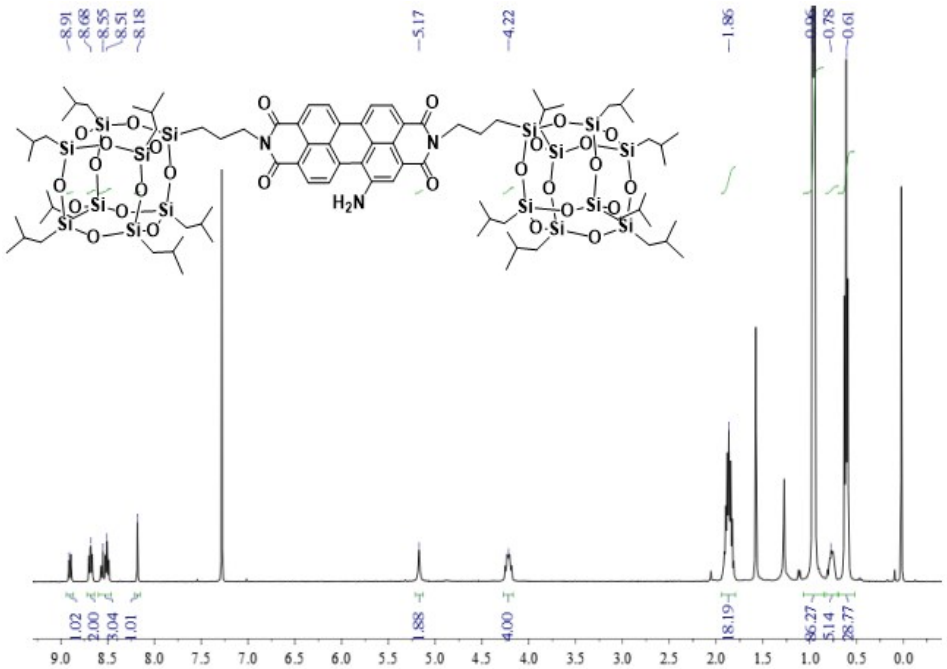

Fig. S13 ^{1}H NMR spectrum of POSS-NH_2PDI recorded in $CDCl_3$.

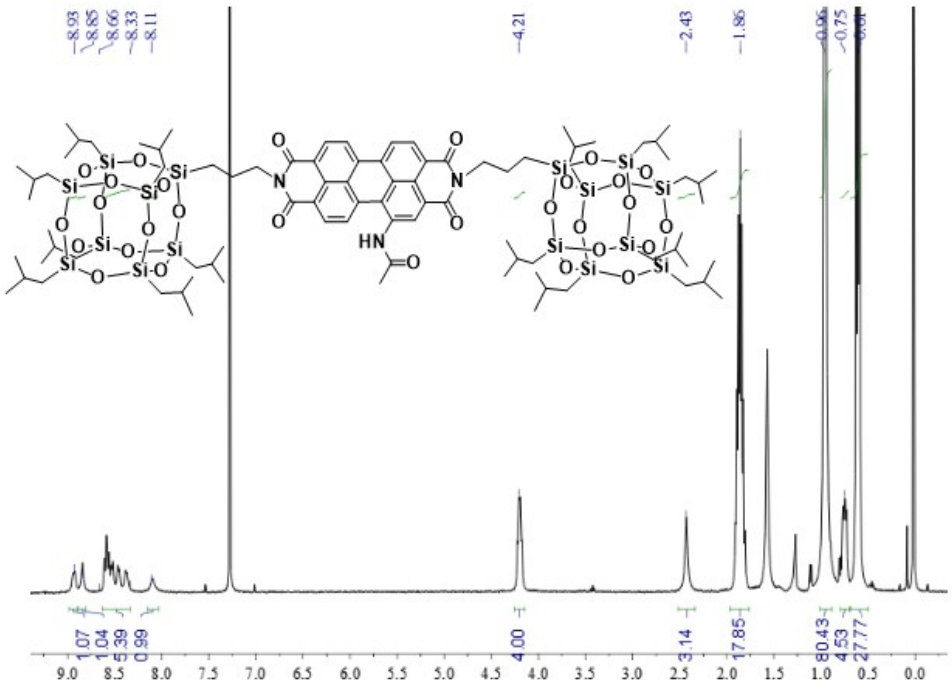

Fig. S14 ^{1}H NMR spectrum of POSS-AMPDI recorded in $CDCl_3$.

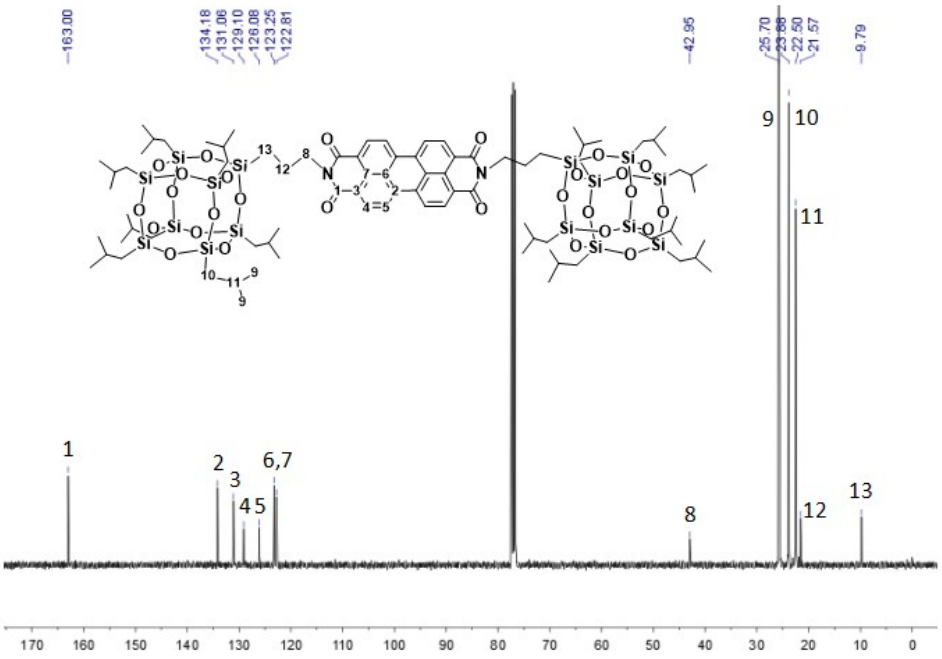

Fig. S15 ^{13}C NMR spectrum of POSS-PDI recorded in $CDCl_3$.

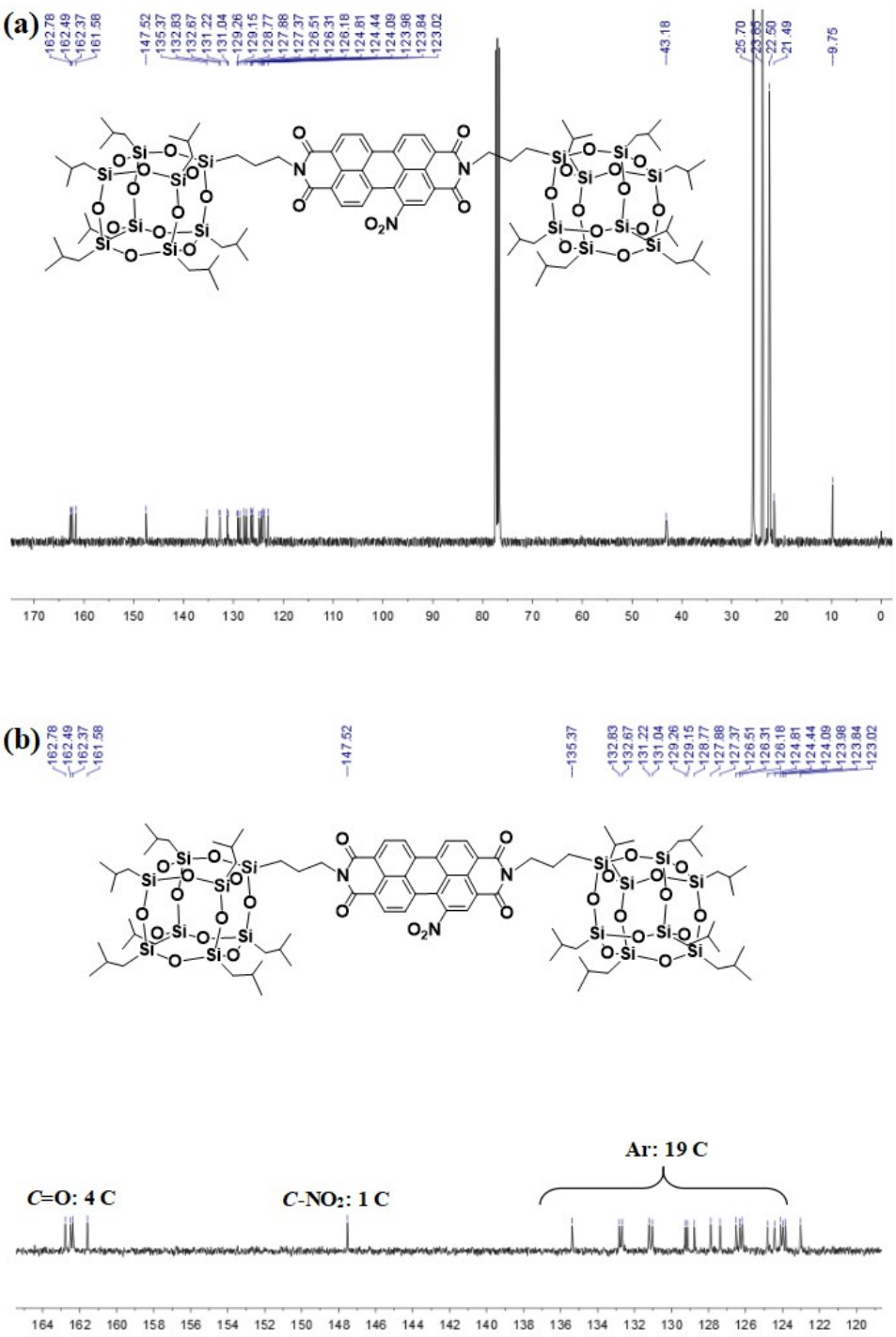

Fig. S16 ^{13}C NMR spectrum of POSS-NO_2PDI recorded in $CDCl_3$. (a) 0-170 ppm; (b) 120-164 ppm.

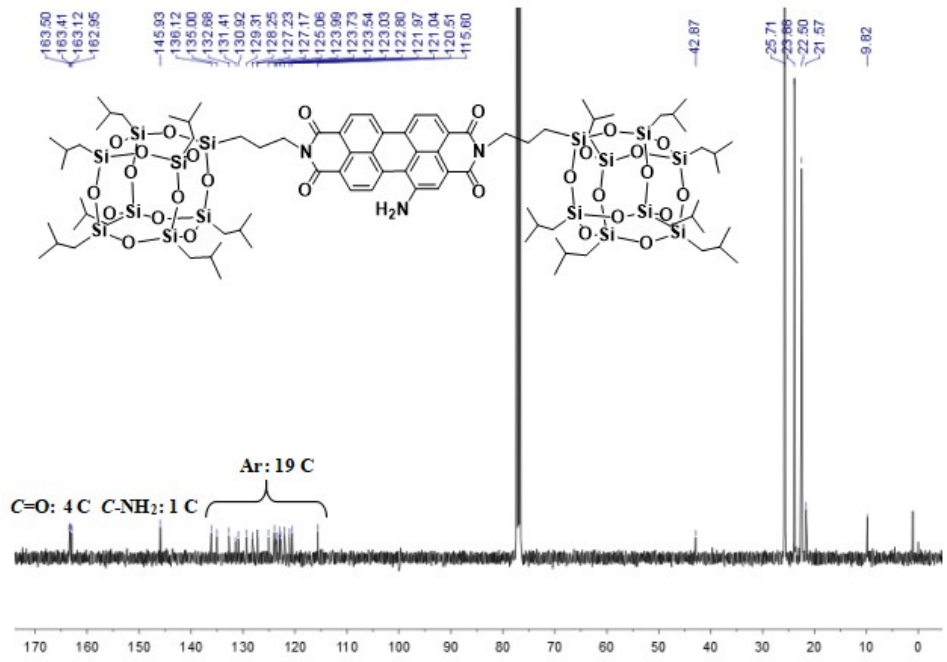

Fig. S17 ^{13}C NMR spectrum of POSS-NH_2PDI recorded in $CDCl_3$.

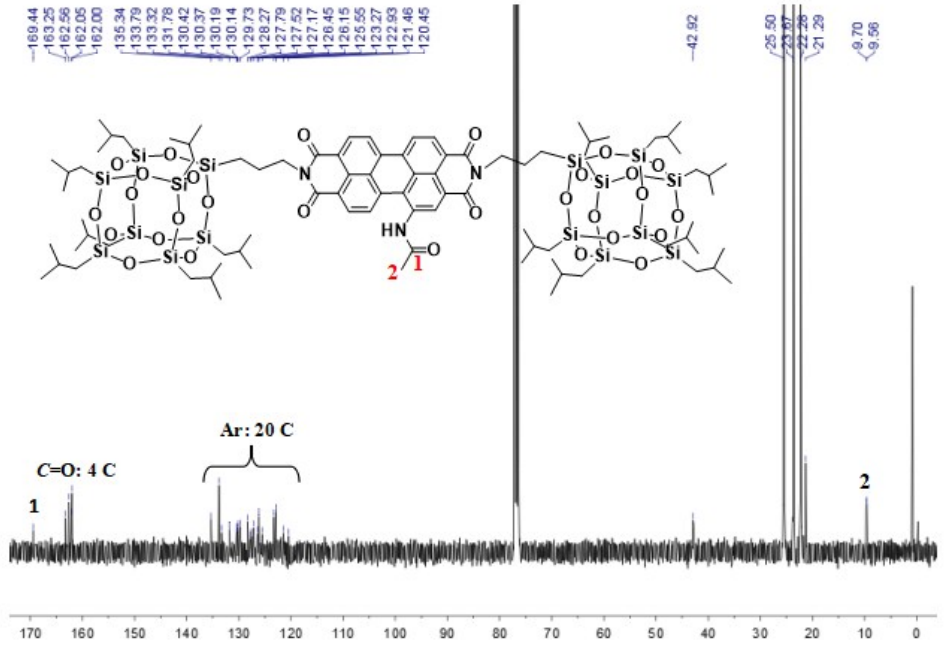

Fig. S18 ^{13}C NMR spectrum of POSS-AMPDI recorded in $CDCl_3$.

Section 9. HRMS (MALDI (N)) Spectra

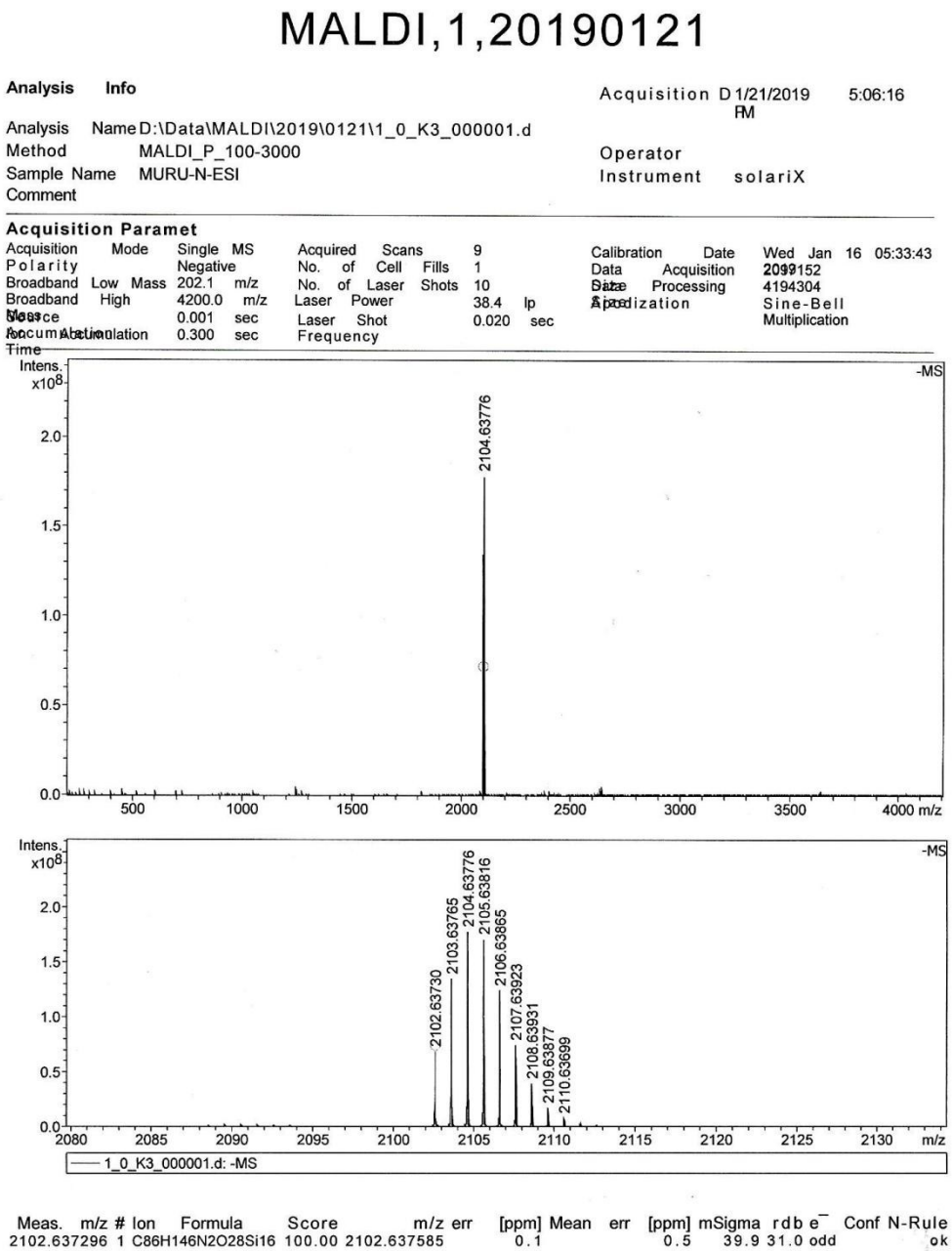

Fig. S19 HRMS (MALDI (N)) spectra of POSS-PDI.

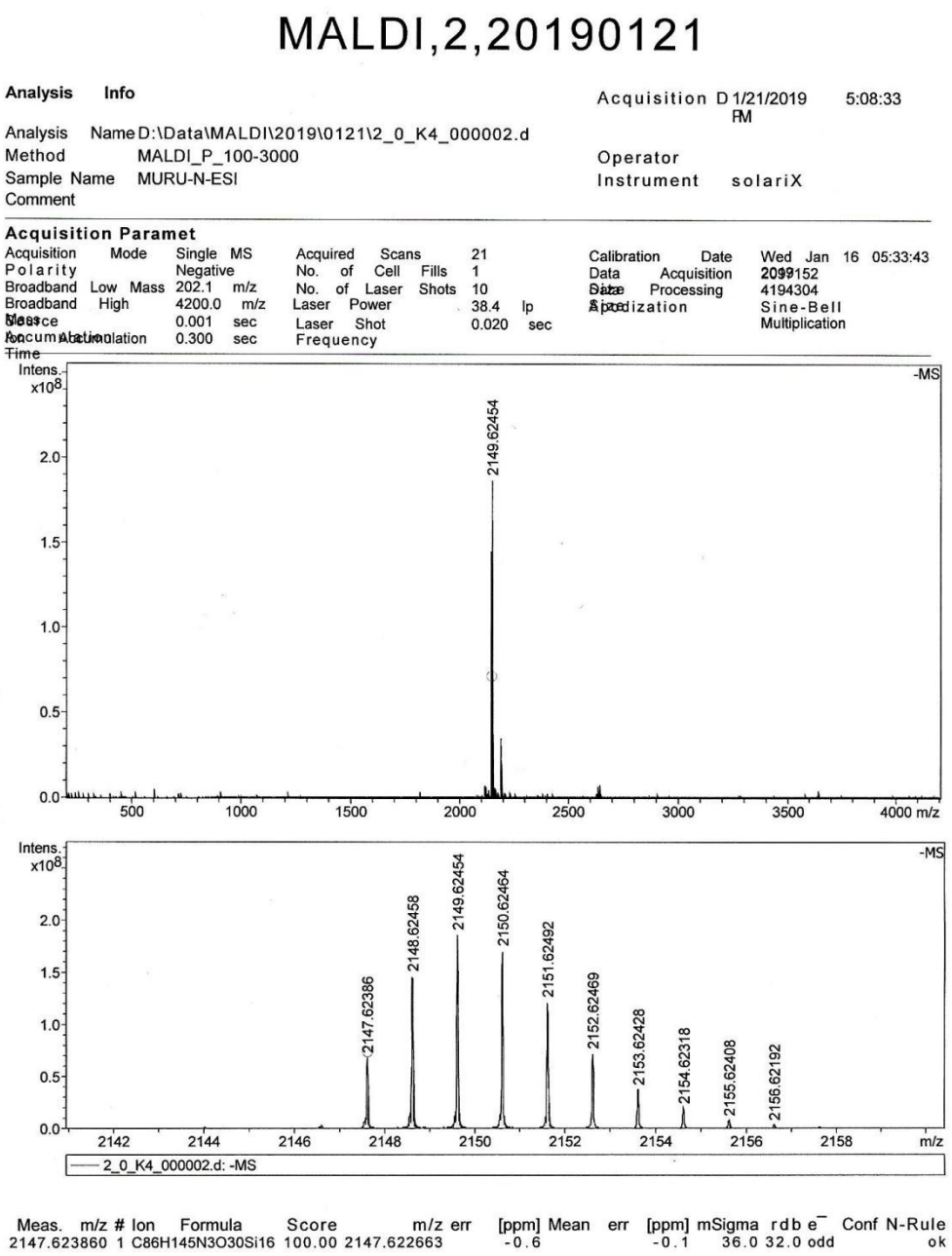

Fig. S20 HRMS (MALDI (N)) spectra of POSS-NO_2PDI.

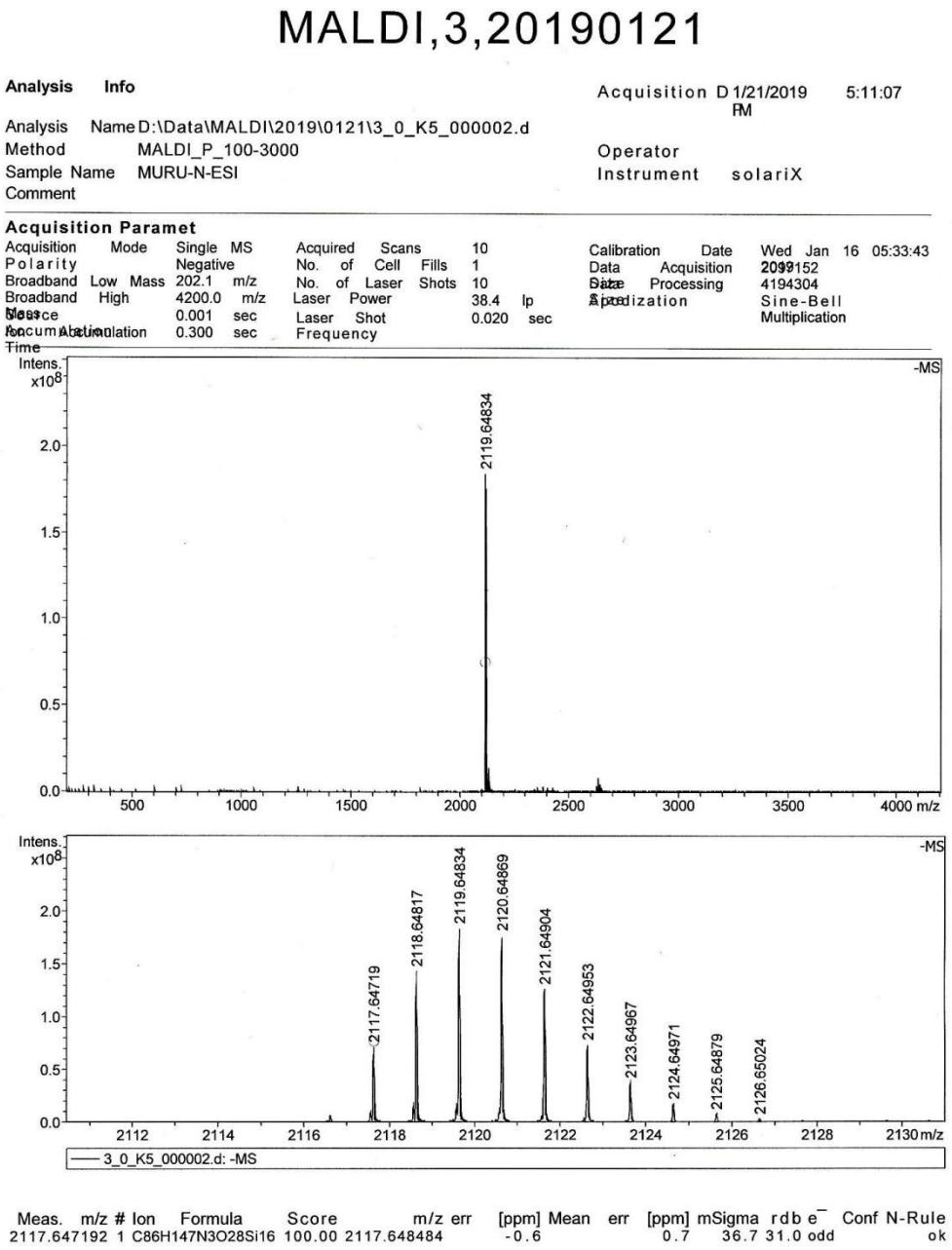

Fig. S21 HRMS (MALDI (N)) spectra of POSS-NH_2PDI.

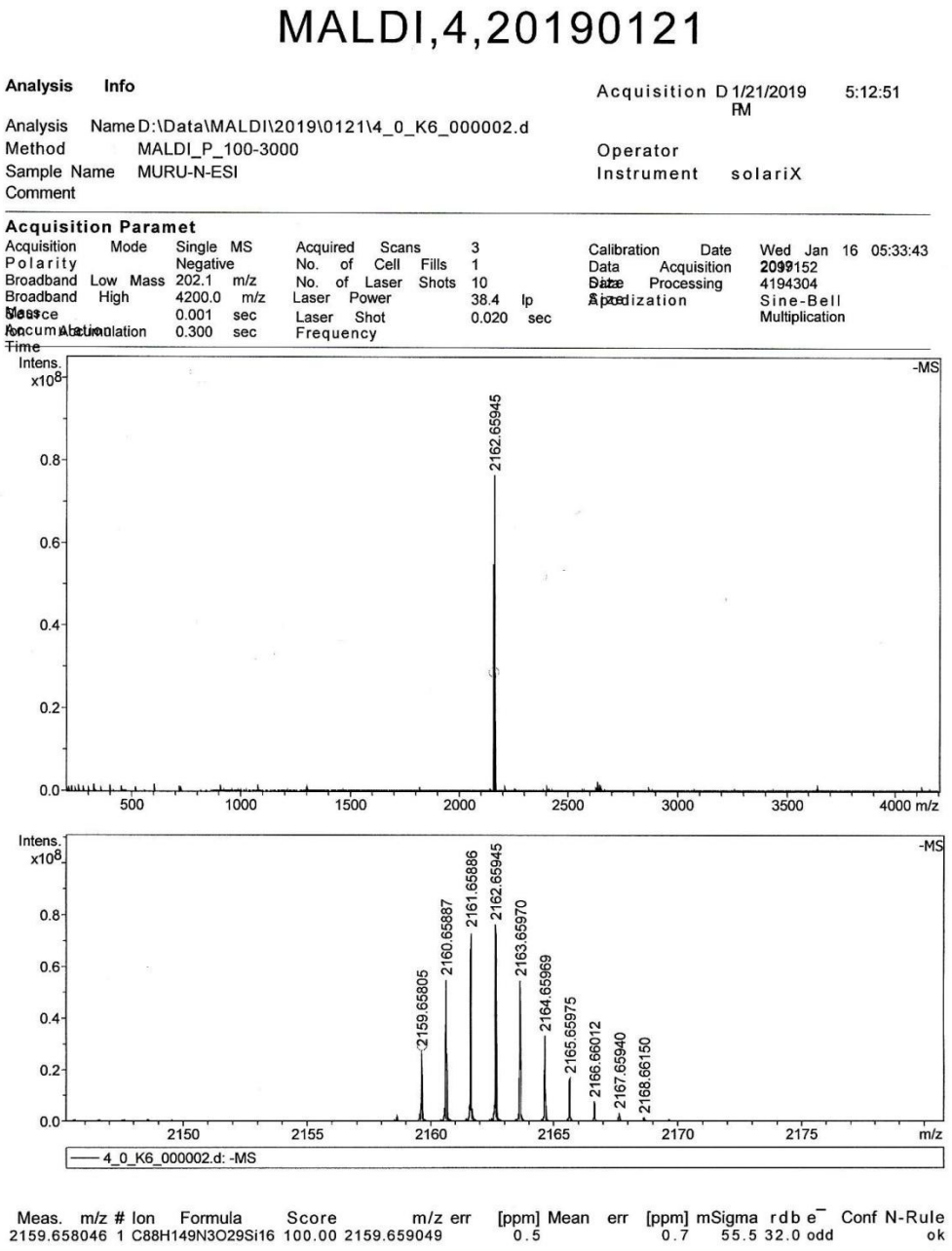

Fig. S22 HRMS (MALDI (N)) spectra of POSS-AMPDI.